

Improvement in Aqueous Solubility of Cilnidipine by Amorphous Solid Dispersion, Its Formulation into Interpenetrating Polymer Network Microparticles and Optimization by Box-Behnken Design

Amit KUHIKAR* , Shagufta KHAN** , Komal KHARABE*** ,
Dilesh SINGHAVI**** , Girish DAHIKAR*****

Improvement in Aqueous Solubility of Cilnidipine by Amorphous Solid Dispersion, Its Formulation into Interpenetrating Polymer Network Microparticles and Optimization by Box-Behnken Design

Silnidipin'in Amorf Katı Dispersiyonu ile Sulu Çözünürlüğünün İyileştirilmesi, Polimer Ağ Mikropartikülleri ile İççe Geçerek Formülasyonu ve Box-Behnken Tasarımıyla Optimizasyonu

SUMMARY

Cilnidipine (CPN), a Biopharmaceutics Classification System class II drug, has dissolution rate-limited bioavailability and a very short half-life (20.4 min). Thus, there is a need to improve the solubility and prolong the drug release so that the therapeutic concentration of CPN could be maintained for a prolonged time. Therefore, the present investigation was aimed to improve the solubility of CPN by preparing amorphous solid dispersion (ASD) and sustain its release by incorporating CPN loaded ASD (CPNASD) in interpenetrating polymer network (IPN) microparticles. ASD was prepared using Solutol HS 15 and Gelucire®50/13. Solutol HS 15 provided a better effect by increasing 84.09 folds solubility of CPNASD in water as compared to the free CPN, therefore it was used in the formulation of IPN microparticles. Characterization of ASD by differential scanning calorimetry (DSC) and X-ray diffraction (XRD) confirmed a decrease in the crystallinity of CPN. IPN microparticles loaded with CPNASD were prepared by varying chitosan concentrations, polyvinyl alcohol (PVA), and mass-ratio of chitosan:TPP and optimized by Box-Behnken Design. The constraints on the responses were maximum drug entrapment efficiency and sustained drug release with more than 80% drug release in 12 h. IPN microparticles with composition, chitosan 50mg, PVA 74.99mg (Volume of aqueous phase; 10 ml, Volume of organic phase; 50 ml) and chitosan:TPP 2.52 was the predicted optimized condition by the software and IPN with this composition provided high % entrapment efficiency (83.87±0.85) and sustained release (83.29±0.55) for 12 h. Solutol HS 15 was successful in providing a massive increase in solubility of CPN, and a uniform sustained release was achieved by loading CPNASD in IPN microparticles.

Key Words: Cilnidipine, Solid dispersion, Solutol HS 15, Interpenetrating polymer network microparticles, Chitosan, Polyvinyl alcohol.

ÖZ

Bir Biopharmaceutics Classification System sınıf II ilacı olan Silnidipin (CPN), çözünme oranıyla sınırlı biyoyararlanıma ve çok kısa bir yarılanma ömrüne (20.4 dakika) sahiptir. O yüzden CPN'nin terapötik konsantrasyonunun uzun bir süre korunabilmesi için çözünürlüğün iyileştirilmesine ve ilaç salımının uzatılmasına ihtiyaç duyulmaktadır. Bu nedenle, halihazırdaki araştırma, amorf katı dispersiyon (ASD) hazırlayarak CPN'nin çözünürlüğünü iyileştirmeyi ve CPN yüklü ASD'yi (CPNASD) iç içe geçen polimer ağı (IPN) mikropartiküllerine dahil ederek salımını sürdürmeyi amaçlamaktadır. ASD, Solutol HS 15 ve Gelucire®50/13 kullanılarak hazırlanmıştır. Solutol HS 15, CPNASD'nin suda çözünürlüğünü serbest CPN'ye kıyasla 84.09 kat artırarak daha iyi etki sağlamıştır, bu nedenle IPN mikropartiküllerinin formülasyonunda kullanılmıştır. ASD'nin diferansiyel taramalı kalorimetri (DSC) ve X-ışını kırınımı (XRD) ile karakterizasyonu CPN'nin kristallikliğinde azalmayı doğrulamıştır. CPNASD ile yüklenmiş IPN mikropartikülleri, farklı konsantrasyonlarda kitosan, polivinil alkol (PVA) ve kitosan TPP kütle oranıyla hazırlanmıştır: ve Box-Behnken Tasarımıyla optimize edilmiştir. Tasarımda cevaplar, maksimum ilaç tutma etkinliği ve 12 saatte %80'den fazla ilaç salımından daha fazla sürekli ilaç salımı ile sınırlandırılmıştır. Yazılım tarafından öngörülen optimize edilmiş kitosan içeren IPN mikropartiküllerinin bileşimi: kitosan 50mg, PVA 74.99mg (Sulu faz hacmi; 10 ml, Organik faz hacmi; 50 ml) ve kitosan : TPP oranı 2.52'dir. Bu bileşimle IPN, yüksek % enkapsülasyon etkinliği (83.87 ± % 0.85) ve 12 saat boyunca sürekli salım (83.29 ± 0.55) sağlamıştır. Solutol HS 15, CPN'nin çözünürlüğünde büyük bir artış sağlamıştır ve CPNASD'nin IPN mikropartiküllerine yüklenmesiyle üniform bir sürekli salım sağlanmıştır.

Anahtar Kelimeler: Silnidipin, Katı dağılım, Solutol HS 15, İç içe geçen polimer ağ mikropartikülleri, Kitosan, Polivinil alkol.

Received: 15.05.2020

Revised: 26.10.2020

Accepted: 31.10.2020

* ORCID: 0000-0001-7353-9814, Institute of Pharmaceutical Education and Research, Bargaon (Meghe) Wardha, Maharashtra, India.

** ORCID:0000-0002-2827-7939, Institute of Pharmaceutical Education and Research, Bargaon (Meghe) Wardha, Maharashtra, India.

*** ORCID: 0000-0002-5237-6929, Institute of Pharmaceutical Education and Research, Bargaon (Meghe) Wardha, Maharashtra, India.

**** ORCID: 0000-0002-2544-7226, Institute of Pharmaceutical Education and Research, Bargaon (Meghe) Wardha, Maharashtra, India.

***** ORCID: 0000-0002-2284-535X, Institute of Pharmaceutical Education and Research, Bargaon (Meghe) Wardha, Maharashtra, India.

INTRODUCTION

Despite sound therapeutic effects, many drugs fail clinically due to their low water solubility, stability, and bioavailability. There are various techniques for enhancing solubility of poorly water-soluble drugs such as particle size reduction, nanosuspension, use of surfactant, salt formation, pH adjustment, hydrotrophy, and solid dispersion (SD) (Sareen et al, 2012).

SD is one of the most effective approaches to improve the solubility and dissolution rate and hence bioavailability of the poorly water-soluble drugs. They release the drug molecularly in the intestinal fluid, generate a supersaturated solution from which the drug moves to the gut wall, permeate, and finally appear in the blood (Guns et al, 2011). Eloy et al, (2012) formulated SD of ursolic acid using Gelucire®50/13 to increase water solubility and bioavailability of ursolic acid. In the present investigation, for ASD, Solutol HS 15 and PEG-32-glycerylpalmitostearate (Gelucire 50/13) were used. Solutol HS 15 (macrogol 15 hydroxystearate, polyoxyl 15 hydroxystearate) is a nonionic solubilizer and emulsifying agent obtained by reacting 15 moles of ethylene oxide with 1 mole of 12 hydroxy stearic acid. (Ruchatz, 1998). Gelucire®50/13 (PEG-32-glycerylpalmitostearate) is water dispersible and reported as a dissolution enhancer and solubilizing agent. It can self emulsify on contact with aqueous media forming a fine dispersion. Its surface active power improves the solubility and wettability of drugs (Panigrahi et al, 2017).

CPN, a BCS class II drug, has dissolution rate-limited bioavailability, so improvement in solubility and dissolution will increase its bioavailability also (Mishra, 2007). CPN also has a short plasma half-life (20.4min), (Uneyama et al, 1999) its conventional dosage forms are unable to control the release of the drug for a prolonged period. Currently, CPN is the most preferred calcium channel blocker among physicians because of its dual blocking characteristics of both L-type voltage-gated Ca^{2+} channels in vascular smooth muscle and N-type Ca^{2+} channels in sympathetic nerve terminals that supply blood vessels. CPN is thus considered a better antihypertensive drug than amlodipine (Lee et al, 2014). However, because of its

extremely short half-life, development an appropriate dosage form that can deliver it in a meaningful manner is highly desirable. Among the various oral controlled release drug delivery systems, IPN microparticles have demonstrated their capability to control the drug release for a prolonged time. There are several investigations on IPN microparticles which support their capability to control drug release. Banerjee et al, (2010) reported that the proper control in the amount of crosslinking agent allowed entrapment of as high as 72% diclofenac sodium and the release for an extended period. Solak, (2011) prepared naproxen loaded IPN microparticles of sodium alginate and polyvinyl alcohol for sustained release. As of now, there is no study involving the use of Solutol HS 15 to improve the solubility of CPN and loading CPNASD in IPN microparticles to achieve high drug loading and prolonged drug release. Therefore, the present investigation is aimed to improve the solubility of CPN by preparing ASD and sustain its release by incorporating CPN loaded ASD (CPNASD) in IPN microparticles containing chitosan and PVA.

MATERIALS AND METHODS

Materials

CPN (J. B. Chemicals and Pharmaceuticals Ltd. Gujrat India), Gelucire®50/13 (Gattefosse India Pvt. Ltd. Mumbai India), Solutol HS 15 (BASF India Pvt. Ltd. Mumbai India), and chitosan (Nitta Gelatin India Pvt. Ltd. Kerala India) were the gift samples. All other chemicals were of analytical grade.

Phase-Solubility Studies

The phase solubility study was performed according to the method reported by Higuchi and Connors (Higuchi and Connors K A, 1965). Excess CPN was added to various concentrations of Gelucire®50/13 (0-1%w/v) or Solutol HS 15 (0-1%w/v) in water. The contents were stirred for 48 h at $37 \pm 0.5^\circ C$ on a magnetic stirrer. After equilibrium, the samples were filtered and analyzed at 232 nm (UV 2401(PC), S.220V Shimadzu Corporation, Japan). The apparent complexation constant $K_{1:1}$ of CPN: Gelucire®50/13 and CPN: Solutol HS 15 was calculated from the slope and intercept of the phase solubility diagrams (Figure not shown), according to the following equation. (Higuchi and Connors, 1965);

$$K_{1:1} = \frac{Slope}{SO(1 - Slope)} \quad (1)$$

Where K 1:1 = apparent complexation constant and SO (intercept) = the solubility of CPN in the absence of the complexing agent.

Preparation of SD

SD of CPN was prepared by the melting method (Rajebahadur et al, 2006). Briefly, CPN was added to molten Gelucire®50/13(MP-50°C, Eloy et al, 2012) / Solutol HS 15(MP-25°C, Rajebahadur et al, 2006). The blend was heated 10°C above the melting point of each carrier for 5 min with stirring. The molten mass was freeze-dried (-20°C and 0.13 bar) for 24 h, crushed and passed through a 500 µm sieve.

Saturation Solubility and In- vitro Dissolution of CPN and SD in Different Media

The saturation solubility of CPN and SD was determined in water, acid buffer pH 1.2, and phosphate buffer pH 6.8 at the ambient temperature (25±2°C). Excess amount of CPN/SD was placed in 20 ml medium in the screw-capped glass vial, stirred for 48 h on a magnetic stirrer at 50 strokes per min, the suspension was then filtered and analyzed spectrophotometrically at 232nm, 241nm, and 244nm for CPN in water, acid buffer, and phosphate buffer

respectively. The standard calibration curve of CPN in water and acid buffer pH 1.2 was linear from 1-10 µg/ml. Equations were $Y = 0.1666 X - 0.0581$; $R^2 = 0.989$ and $Y = 0.1653 X - 0.0851$; $R^2 = 0.995$ for water and acid buffer respectively. The calibration curve of CPN in phosphate buffer was linear in the concentration range of 1-5 µg/ml with $R^2 = 0.991$ and equation $Y = 0.1802 X - 0.1607$. LOQ of CPN in water, acid buffer and phosphate buffer were 0.1, 0.3, and 0.03 µg/ml respectively. For analysis of intra-day and inter-day variability, a triplicate of curve was studied, and % RSD was calculated. Percent RSD was less than 5% in each case (Pinto et al, 2017). The dissolution was done in the 500 ml (Crist, 2009) of the same media as solubility using the USP type I apparatus at 50 rpm and 37±0.5°C. 10 mg CPN or SD equivalent to 10 mg were used for the study. A 3 ml sample was withdrawn at the predetermined time intervals and analyzed spectrophotometrically (Table1).

Drug Content of SD

Fifty milligram SD was dispersed in 50 ml DMSO, stirred for 24 h at 25±0.5°C on a magnetic stirrer at 50 strokes/min, filtered, and analyzed spectrophotometrically at 261 nm.

Table 1. Saturation solubility and dissolution of CPN, CPN- Gelucire®50/13SD and CPN- Solutol HS 15 SD in different media

Mean Saturation Solubility of CPN*(mg/ml) at 25 ± 0.5 °C				Solubility Enhancement Ratio	
Media	Free drug	Solid dispersion CPN : Gelucire®50/13 (1:1)	Solid dispersion CPN : Solutol HS 15 (1:1)	Solid dispersion CPN : Gelucire®50/13 (1:1)	Solid dispersion CPN : Solutol HS 15 (1:1)
Water	0.002±0.01	0.026±0.01	0.185±0.03	12.22	84.09
Acid buffer pH 1.2	0.013±0.02	0.028±0.05	0.319±0.09	02.19	24.54
Phosphate buffer pH 6.8	0.040±0.02	0.088±0.02	0.579±0.06	02.20	14.47

*n=5±S.D

Solid State Characterization of SD by FTIR, DSC and XRD

The potassium bromide disc containing CPN, polymer, and their physical mixture were scanned in the range of 4000 to 400 cm⁻¹ using an FTIR spectrophotometer (Model- 84005, Shimadzu Asia Pacific Pvt. Ltd. Singapore) (Figure 1A). For DSC, 5-10 mg samples sealed in an aluminum pan were scanned at a rate of 10°C/min between 30 to 300°C (Model -DSC 60, Shimadzu, Tokyo, Japan). A nitrogen

purge (20ml/min) was maintained using an empty sealed pan as reference. Temperature and heat flow calibrations were performed using indium as standard (Figure 1B). X-ray diffraction measurements were done (Smartlab, Rigaku Corporation, Tokyo, Japan) with a copper anode operating under CuK radiation (1.5406 Å, 45kV, and 40mA). Patterns were obtained using a step width of 0.05°/s from 2° to 50° at room temperature on a 2θ scale (Figure 1C).

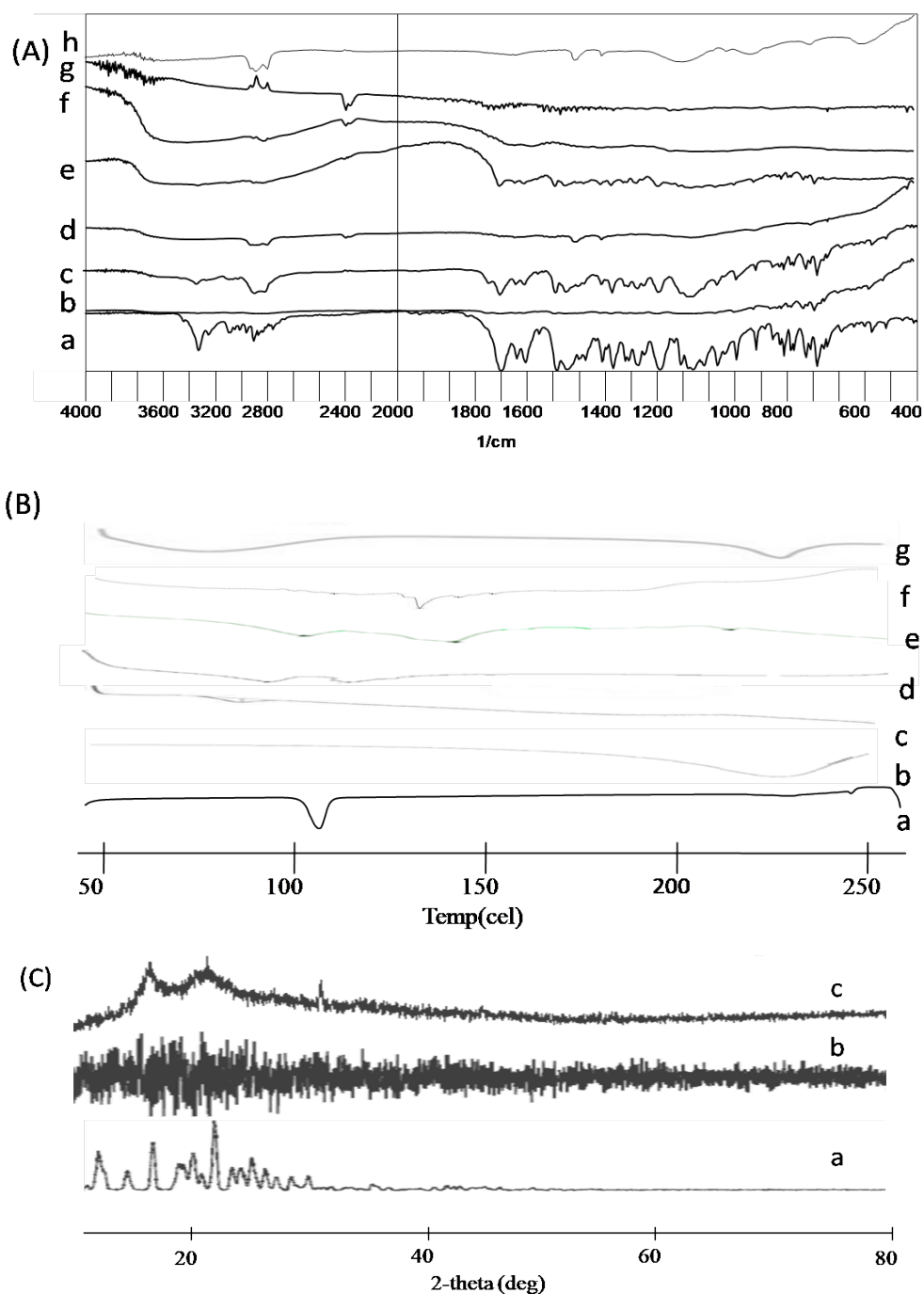


Figure 1. A) FTIR of (a) CPN (b) CPN **Gelucire**[®]50/13SD. (c) CPN **Solutol HS 15** SD (d) IPN microparticles (e) Physical mixture containing CPN, chitosan and PVA (f) Chitosan (g) PVA (h) Blank IPN microsphere B) DSC of (a) CPN (b) PVA (c) Chitosan (d) CPN- **Solutol HS 15** SD (e) Physical mixture containing CPN, chitosan and PVA (f) IPN microparticles g) Blank IPN microsphere C) XRD of (a) CPN (b) IPN microparticles (c) SD of CPN with **Solutol HS 15**

Preparation of IPN microparticles

SD with Solutol HS 15 gave substantially greater solubility and dissolution rate than Gelucire[®]50/13, therefore it was used for the preparation of microparticles. Microparticles were prepared by the

emulsion crosslinking method (Bulut et al, 2014). Briefly, to a mixture of chitosan solution (in 1% aq. acetic acid) and polyvinyl alcohol solution (in warm water), SD equivalent to CPN 30 % (w/w) of the

polymer was added and after that, the aqueous phase (10 ml) was added drop-wise via 22-gauge hypodermic needle into 50 ml light liquid paraffin containing 1% span 80 and homogenized at 3000 rpm for 20 min. To this, the crosslinker sodium tripolyphosphate solution (STPP) was added with homogenization at 3000 rpm for one hour. The microparticles were separated by centrifugation, washed several times with n-hexane to remove liquid paraffin, and freeze-dried (-20°C and 0.13 bar for 24 h). Different batches

of IPN microparticles were prepared and optimized using Box Behnken Design (Drug design expert 11 software). The independent variables were the amount of chitosan (low 50 mg and high 100 mg), PVA (low 50 mg and high 100 mg), and chitosan : STPP (low 2.5 and high 3) while, the dependent variables were entrapment efficiency and cumulative percent drug release in 12 h (Table 2). For optimization, constraints on responses were maximum entrapment efficiency, and more than 80% cumulative drug release in 12 h.

Table 2. Composition of IPN microparticles according to Box Behnken Design using Drug Design Expert 11 software.

Run	Batch	Factor 1 Chitosan (mg)	Factor 2 Polyvinyl alcohol (mg)	Factor 3 Chitosan: STPP	% EE	% Drug Release in 12 h
1	IPN 1	75	75	2.75	64.12±0.50	67.67±0.75
2	IPN 2	100	50	2.75	59.04±0.54	60.63±0.45
3	IPN 3	50	75	3	75.15±0.43	75.04±0.85
4	IPN 4	100	100	2.75	63.73±0.85	65.96±0.95
5	IPN 5	50	100	2.75	73.25±0.65	78.08±0.45
6	IPN 6	50	50	2.75	74.66±0.55	73.42±0.35
7	IPN 7	75	100	2.5	65.88±0.85	67.41±0.55
8	IPN 8	100	75	3	54.02±0.35	64.08±0.65
9	IPN 9	75	50	3	64.10±0.25	74.02±0.25
10	IPN 10	75	50	2.5	66.16±0.65	71.67±0.65
11	IPN 11	100	75	2.5	62.63±0.50	62.66±0.75
12	IPN 12	50	75	2.5	83.87±0.85	83.29±0.55
13	IPN 13	75	100	3	63.95±0.75	62.63±0.89
14	IPN1	75	75	2.75	64.12±0.25	67.67±0.98
15	IPN1	75	75	2.75	64.12±0.35	67.67±0.65
16	IPN1	75	75	2.75	64.12±0.35	67.67±0.75
17	IPN1	75	75	2.75	64.12±0.55	67.67±0.55

Volume of aqueous phase; 10 ml, Volume of organic phase; 50 ml n=3±S.D

Drug Loading Capacity, EE, Particle Size, Solid State Characteristics, Particle Morphology and Water Uptake of Microparticles

Hundred mg microparticles were crushed, soaked

in 100 ml of DMSO for 24 h and after filtration. analyzed at 261 nm. Drug loading capacity and entrapment efficiency (Table 2 and 3) were calculated using the following equation:

$$\text{Drug Loading Capacity} = \frac{\text{amount of drug entrapped in microparticles}}{\text{weight of microparticles}} \times 100 \tag{2}$$

$$\% \text{Entrapment Efficiency} = \frac{\text{Actual drug content}}{\text{Theoretical drug content}} \times 100 \tag{3}$$

A hundred particles were measured by the Imaging system (Metzger Optical Instrument, no. 666 Mathura, India), and the average was determined (Siepmann et al, 2005) (Table 3). To evaluate the

particle size distribution, polydispersity index (PI) (Table 3) was calculated using the equation;

$$PI = \frac{D(0.9) - D(0.1)}{D(0.5)} \tag{4}$$

Where, D (0.9), D (0.5), and D (0.1) corresponds to particle size immediately above 90%, 50%, and 10% of the sample (Viveksarathi and Kannan, 2015). Solid-state characteristics of microparticles were studied by FTIR, XRD, and DSC in the same way as CPN and SD. For morphology, microparticles were coated with platinum and visualized under a scanning electron

microscope (Model S-3700N, Hitachi, Japan) (Figure 2). For water uptake, microparticles were swollen in the acid buffer pH 1.2 for 2h and phosphate buffer pH 6.8 for 10 h, were blotted off with tissue paper to remove excess water and weighed (Reddy and Nagabhushnam 2017)(Table 3).

$$\text{Percent water uptake} = \frac{\text{Mass of swollen microparticles} - \text{Mass of dry microparticles}}{\text{Mass of dry microparticles}} \times 100 \quad (5)$$

Table 3. Drug content, Diameter and Water Uptake of IPN microparticles

Batches	Drug Loading Capacity ^a (%)	Mean Diameter ^b (Micron)	Polydispersity Index	% Equilibrium water uptake ^a	
				Acid buffer pH 1.2 (For 2 h)	Phosphate buffer pH 6.8 (For 10 h)
IPN 1	11.62±0.35	21.87±4.65	0.52	174.96±0.85	399.49±0.95
IPN 2	10.70±0.25	19.35±3.85	0.48	156.34±0.90	369.81±0.85
IPN 3	13.62±0.35	25.72±3.51	0.45	199.61±0.65	423.00±0.65
IPN 4	11.55±0.45	25.74±5.23	0.55	171.32±1.20	371.13±0.89
IPN 5	13.27±0.25	24.94±3.51	0.43	184.91±1.20	389.31±1.25
IPN 6	13.53±0.30	21.25±2.15	0.37	179.43±1.35	395.09±1.35
IPN 7	11.92±0.40	18.88±3.23	0.47	181.62±0.85	377.87±1.45
IPN 8	09.79±0.26	23.81±4.92	0.51	161.40±0.75	383.56±0.98
IPN 9	11.98±0.30	24.12±3.55	0.46	163.69±0.93	349.63±0.65
IPN 10	11.99±0.75	18.40±3.42	0.44	201.54±1.23	411.41±0.65
IPN 11	11.35±0.43	18.56±3.62	0.49	174.33±1.32	361.08±0.95
IPN 12	15.20±0.25	21.23±4.22	0.51	189.31±1.23	406.91±0.86
IPN 13	11.59±0.27	26.19±3.75	0.48	170.39±1.25	381.43±0.95

a.n=3 ± S. D, b.n=100 ± S. D

In-Vitro Drug Release

Drug release was investigated initially for 2h in the acid buffer pH 1.2 and then 10 h in phosphate buffer pH 6.8 using USP Type I apparatus, at 100 rpm. Microparticles, equivalent to 10 mg of CPN were added in 500 ml dissolution medium at 37°C±0.5°C. Samples were withdrawn at a predetermined time and analyzed at 241nm for acid buffer and 244 nm for phosphate buffer, respectively (Figure 6). Drug release profiles were modeled with different kinetic equations like Higuchi, (Higuchi, 1963) first-order and zero-order (Costa et al, 2003) to know the kinetics of drug release and to elucidate the mechanism of drug release, Korsmeyer Peppas (Peppas, 1985) equation was used.

Zero-order release equation:

$$Qt = K_0.t \quad (6)$$

First-order equation:

$$\ln Qt = \ln Q_0 - k_1.t \quad (7)$$

Higuchi equation:

$$Qt = kH.t \frac{1}{2} \quad (8)$$

Qt is the amount of drug released in time t; Q₀ is the initial amount of drug; and k₀, k₁, and kH are the rate constants of the zero-order, first-order, and Higuchi equations, respectively.

Korsmeyer Peppas equation:

$$\frac{Mt}{M_\infty} = kt^n \quad (9)$$

Mt is the amount of drug released at time t, and M_∞ is the amount released at time t = ∞. Thus Mt/M_∞ is the fraction of drug released at time t, k is the kinetic constant, and n is the diffusion exponent.

Stability Study

Stability study was carried out by storing the microparticles (wrapped in aluminum foil) at $40 \pm 5^\circ\text{C}$ and $75 \pm 5\%$ RH for 6 months. At an interval of 1 month, the microparticles were visually examined for any physical change, drug loading capacity, particle size, and in-vitro drug release.

RESULTS AND DISCUSSION

Phase Solubility, Saturation Solubility and In-vitro Dissolution of CPN and SD

The phase solubility curve of CPN in presence of Gelucire[®]50/13 and Solutol HS 15 showed linear increase in CPN solubility with the concentration of Gelucire[®]50/13 (AL Type, $y = 0.0011x + 0.002$, $R^2 = 0.986$) and Solutol HS 15 (AL Type, $y = 0.002x + 0.0015$, $R^2 = 0.995$) (Figure not shown). K1:1 of CPN- Solutol HS 15 SD was found to be 2.72 mM, while that of CPN- Gelucire[®]50/13 was 1.11mM. Solutol HS 15 was more effective at increasing solubility of CPN (84.09 times solubility of free CPN in water) as compared to Gelucire[®]50/13 (Table 1). The improvement in solubility by Solutol HS 15 was statistically significant with $p < 0.05$ (two-tailed $p = 0.0079$, unpaired t-test-Mann-Whitney test). The dissolution of CPN was higher in both acid buffer pH 1.2 and phosphate buffer pH 6.8 from CPN Solutol HS 15 SD. At 4h, there was a 3.27 and 2.79 folds increase in CPN release from SD having Solutol HS 15 in acid and phosphate buffer, respectively, compared to the free CPN.

Solid State Characterization of SD by FTIR, DSC and XRD

FTIR of CPN revealed characteristic peaks at 1566.09 cm^{-1} , 3288.40 cm^{-1} and 1697.24 cm^{-1} due to NC group stretching, aromatic stretching, and C=O group stretching respectively. (Figure 1A) The DSC of CPN displayed a sharp endothermic peak at 113.5°C due to its melting. However, the melting peak of the drug was broad with reduced intensity in SD (Figure 1B). XRD of CPN exhibited characteristic, intense

peaks at 2θ of 18.81° , 20.29° , and 24.08° that were absent in SD. (Figure 1C)

Drug Loading Capacity, EE, Particle size, Solid State Characteristics, Particle Morphology and Water Uptake of Microparticles

Drug loading capacity ranged from 9.79 ± 0.026 to $15.20 \pm 0.27\%$ while EE was between 54.02 ± 0.12 and $83.87 \pm 0.29\%$. EE was found dependent on the amount of chitosan, PVA, and chitosan:STPP. The polynomial equation correlating EE with independent variables is;

$$\% EE = 60.30 - 8.44 * A + 0.3563 * B - 2.67 * C \quad (10)$$

Where A and B are the amount of chitosan, and PVA and C is the chitosan:STPP ratio.

The Model F-value of 20.06 and $P < 0.0001$ implied that the model was significant. Effect of chitosan, PVA, and chitosan : STPP on EE is displayed by the response surface diagram (Figure 3Bi). The particle size of microparticles ranged from 18.40 ± 3.42 - $26.19 \pm 3.75\ \mu\text{m}$ and found dependent on the concentration of polymer and crosslinker. PI was found in the range of 0.37-0.55. FTIR spectrum of IPN microparticles showed no change in the chemical structure of CPN as there was no difference in the fingerprint region of the drug. (Figure 1A). DSC of IPN microparticles showed a broad endothermic peak at a higher temperature (143.4°C) (Figure 1B). The characteristic sharp peaks of CPN had disappeared in the XRD of microparticles (Figure 1C). Scanning electron microscopic photographs revealed discrete microparticles with rough surfaces. The microparticles were slightly irregular in shape but mostly uniform in size. (Figure 2a and b). The percent equilibrium water uptake after 12 h was between 349.63 ± 0.65 and $423.0 \pm 0.65\%$. The formulations containing a higher amount of PVA increased the equilibrium water uptake.

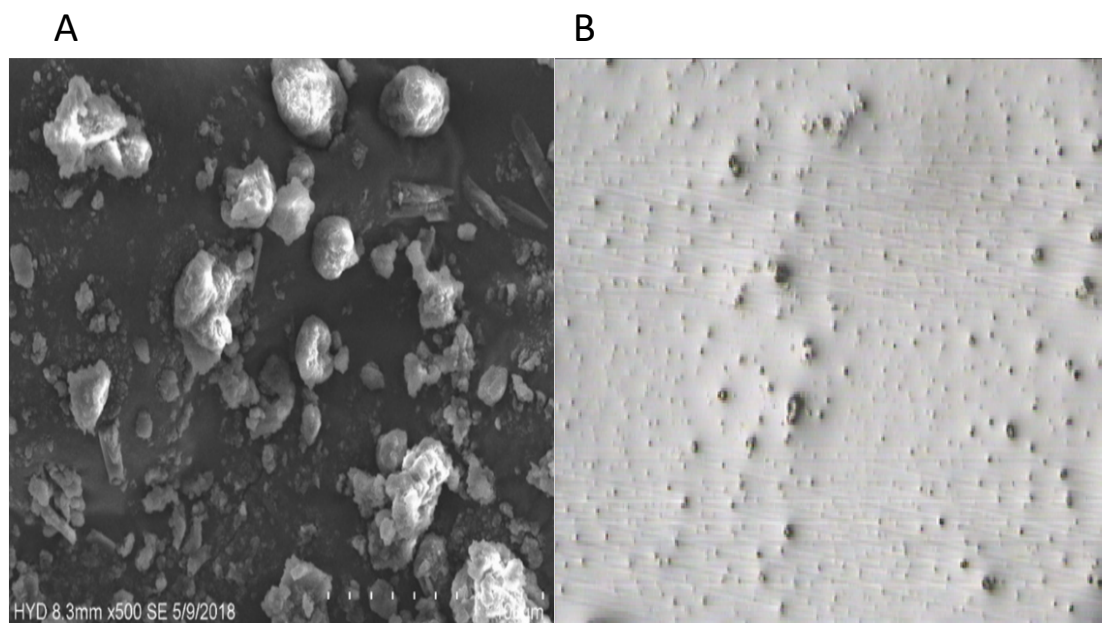


Figure 2. A) Scanning electron micrograph of IPN microparticles B) Image of particles taken by Metzger Optical Instrument at 100X magnification

In-Vitro Drug Release

The cumulative release ranged from 60.63 ± 0.04 to 83.29 ± 0.055 % in 12 h (Figure 3A). The variance in drug release was due to differences in the level of PVA /chitosan and chitosan: STPP in formulations. The polynomial equation relating percent drug release with independent variables was found as;

$$\% \text{ Cumulative Drug Release} = 69.25 - 7.06 * A - 0.7075 * B - 1.16 * C \quad (11)$$

The Model F-value of 11.51 and $P < 0.0006$ indicated that the model was significant. Effect of chitosan, PVA, and chitosan: STPP on drug release is displayed by the response surface diagram (Figure 3Bii). With the increase in the level of PVA, CPN release increased. R^2 was maximum for zero-order kinetics for all formulations (ranged from 0.96-0.99) and slope of Koresmeyer Peppas equation was ≥ 0.85 -(ranged from 0.85 to 1.06).

Optimization by Desirability Function

Optimization was done by desirability function. CPNASD loaded microparticles prepared under optimized condition (chitosan 50 mg, PVA 74.99 mg (aqueous phase; 10 ml and organic phase; 50 ml) and chitosan:TPP2.52) displayed responses (% EE; 83.87 ± 0.85 and % CPN release in 12 h; 83.29 ± 0.55) very

close (low % bias) to predicted responses (% EE; 83.35 and % CPN release in 12 h; 83.05) confirming the reliability of the model.

DISCUSSION

Saturation Soubility and In-vitro Dissolution of CPN and SD

Due to high hydrophilicity, remarkable wetting ability, and low CMC (0.005 % to 0.02%), Solutol HS 15 has excellent capability to form micelles and entrap drugs. Also, with more homologation series, it creates more hydrogen bonding than Gelucire®50/13, giving greater solubility and dissolution of CPN. High CPN release from SD could be due to loss of crystal structure of CPN in SD (Ádley et al, 2008). Rapid dissolution was because of the molecular dispersion of CPN in SD. Because of the molecular dispersion of CPN in SD, the greater surface area was exposed to the medium (Cid et al, 2019). An increase in the dissolution rate of CPN from SD compared to the plain drug can also be attributed to the amorphization and loss of crystal structure of the drug upon the formation of solid dispersion (Cid et al, 2019).

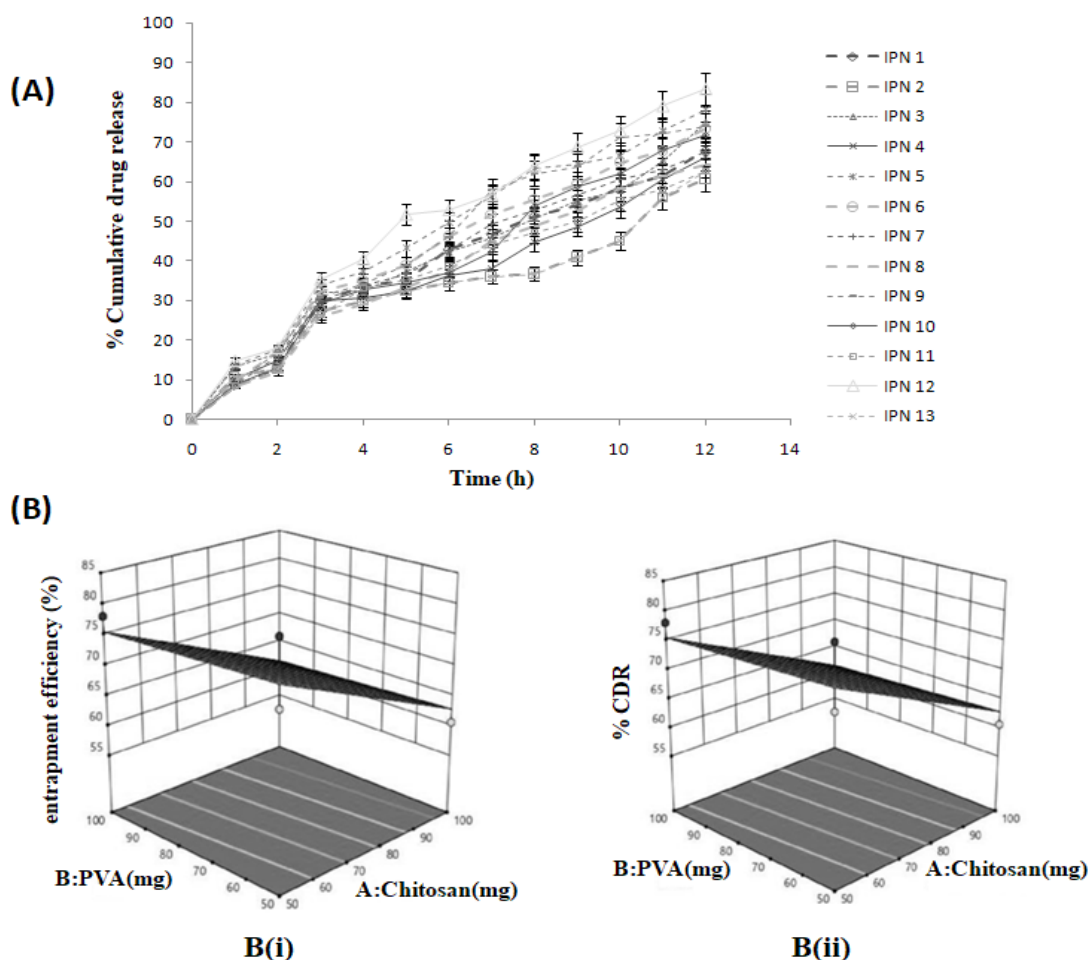


Figure 3. A) In-vitro drug release study of CPN from IPN microparticles (n=3,S.D<±1%)B)Contour and 3D surface graphs showing effect of chitosan, PVA and chitosan:TPP on (i)% entrapment efficiency (ii) cumulative drug release

Solid State Characterization of SD by FTIR, DSC and XRD

No change in the characteristic peaks of CPN was noted in the FTIR of SD, which signifies that there was a lack of interaction between CPN and carriers. The broadening of the endothermic peak of CPN in DSC confirms the loss of crystallinity of CPN in SD. The absence of characteristic sharp intense peaks of CPN in XRD further confirms the loss of crystallinity of CPN and it could be inferred that it is dispersed at the molecular level in the solid dispersion.

Drug Loading Capacity, EE, Particle Size, Solid State Characteristics, Morphology and Water Uptake of Microparticles

As the level of chitosan increased, dense

microparticles due to the high crosslinked density of polymer matrix were formed which enabled them to hold a high amount of drug (Sedyakina et al, 2018). At the intermediate level of PVA, EE was high because PVA helped maintain the viscosity and retain the drug, but higher PVA level had a negative impact on EE as very high viscosity reduced access of STPP to chitosan, causing poorly crosslinked, loose network with reduced capacity to hold the drug. STPP level helped to form a tightly networked structure to hold CPN, however with too high STPP (chitosan: STPP,2.5) EE decreased due to the constriction of microparticles and expulsion of drugs (Hou et al, 2015). Increase in the chitosan: STPP above 2.7 increased the particle size of microparticles because of the shortage of

STPP for crosslinking chitosan, which produced a loose network, while at a lower ratio rigidization of chitosan resulted in shrinking of particles to lower size (Patel and Patel M, 2014). Because of the entrapment of CPN in the microparticles, there could be hindered melting, so the endothermic peak shifted to a higher temperature in the DSC of microparticles. The broadening of the peak was due to a reduction in crystallization and entrapment of CPN at the molecular level in the microparticles (Sharma, 2010), which is corroborated by the absence of peaks in XRD of microparticles (Karavelidis et al, 2011).

Particles had a rough surface because of the crosslinking of chitosan and drug's loading (Long et al, 2019). Particles were of uniform size as PI was near 0.5 or less. PI less than 0.5 is deemed homogeneous, while PI > 0.7 is considered to be in a very broad size range (Mudalige et al, 2019). Water uptake capacity increased with PVA because of its high hydrophilicity and excellent water absorption. At the high concentration of chitosan in the microparticles, the swelling was decreased due to the rigid, low water absorbing network formed at the higher chitosan concentration.

In-Vitro Drug Release

A high amount of chitosan caused reduced drug diffusion due to the rigid microsphere network. With the increase in the level of PVA in the IPN microparticles, CPN release increased because of the hydrophilicity of PVA, greater absorption of water, and loose network of microparticles in the presence of a high amount of PVA. However, at the high level of STPP, rigid, compact microparticles were produced, which retarded the drug release (Kaushik et al, 2015). Drug release occurred by diffusion through the swollen matrix and chain relaxation at later time points due to waning crosslinks which aided sufficient drug release at the later time points too. As the slope of the Korsmeyer Peppas equation was greater than 0.85 for each formulation batch, a case-II (zero-order) drug-release mechanism was dominant (Sarfaraz et al, 2010).

Stability Study

CPNASD loaded IPN microspheres prepared under the optimized condition suggested by the experimental model was found to be stable with insignificant change (unpaired t-test, $p < 0.05$) in drug loading capacity and percent drug release when stored under $45 \pm 5^\circ\text{C}$ and $75 \pm 5\%$ RH for 6 months (Table 4).

Table 4. Drug loading capacity, particle size, and in-vitro drug release of microparticles* placed at $40 \pm 5^\circ\text{C}$ and $75 \pm 5\%$ RH for 6 months stability testing

Time (Months)	Drug Loading Capacity ^a (%)	% EE ^a	Mean Diameter ^b (Micron)	% CPN release in 12 h ^a
0	15.20±0.25	83.87 ±0.85	21.23±4.22	83.29±0.55
1	14.95±0.12	82.50±0.65	21.45±4.50	83.57±0.75
2	15.28±0.23	84.32±1.25	21.35±5.15	83.45±0.95
3	15.45±0.09	85.26±0.45	21.85±5.0	84.15±1.5
4	14.80±0.06	81.67±0.35	21.75±4.55	83.95±1.35
5	15.12±0.17	83.44±0.95	21.50±4.85	83.75±0.75
6	14.98±0.27	83.67±1.5	21.80±4.9	84.05±1.8

a.n=3 ± S. D, b.n=100 ± S. D *Microparticles were prepared under optimized condition (chitosan 50 mg, PVA 74.99 mg (aqueous phase; 10 ml and organic phase; 50 ml) and chitosan:TPP2.52).

CONCLUSION

Solutol HS 15 was successful in improving the solubility of CPN because of which unhindered drug release over a prolonged period was accomplished from the IPN microparticles. Thus CPNASD loaded IPN microparticles could address both the solubility and short biological half-life concern of CPN. As Solutol HS 15 retained CPN within the core of the micelle, there was low seepage of the drug during

microsphere formation due to the crosslinking of chitosan chains, which was the reason for high drug entrapment in microparticles. Else, the expulsion of the drug during crosslinking of polymer and microsphere formation is the common cause for low drug entrapment. Thus, the presented results provided a new possibility for the successful delivery of a highly therapeutically important drug candidate having poor solubility as well as short elimination half-life.

CONFLICT OF INTEREST

The authors declare that there are no conflicts of interest.

AUTHOR CONTRIBUTION STATEMENT

Performed experiments (Kuhikar A.), mentor, hypothesis, design, manuscript preparation, framed discussion of the manuscript (Khan S.), writing manuscript, literature research (Kharabe K.), preparing figures, writing manuscript (Singhavi D.), interpretation of FTIR, discussion confirming formation of interpenetrating polymer network (Dahikar G.)

REFERENCES

- Banerjee, S., Chaurasia, G., Pal, D.K., Ghosh, A.K., Ghosh, A., Kaity, S. (2010) Investigation on cross-linking density for development of novel interpenetrating polymer network (IPN) based formulation. *Journal of Scientific and Industrial Research*, 69, 777-784.
- Bulut, E. (2014). In-vitro evaluation of ibuprofen loaded microparticles prepared from novel chitosan-polyvinyl alcohol interpenetrating polymer network. *Polymer Plastic Technology and Engineering*, 53, 371-378.
- Cid, A.G., Simonazzi, A., Palma, S.D., Bermudez J.M. (2019) *Therapeutic Delivery*, 10(6),363-381.
- Costa, F.O., Sousa, J.J., Pais, A.A., Fornosinho, S.J. (2003) Comparison of dissolution profile of ibuprofen pellets. *J. Control. Release*, 89, 199-212.
- Crist, G.B. (2009). Trends in small-Volume Dissolution Apparatus for Low-Dose Compounds. *Dissolution Technologies*, 16(1), 19-22.
- El-Feky, G.S., El-Rafie, M.H., El-Sheikh, M.A., El-Naggar, M.E., Hebeish, A. (2015). Utilization of Crosslinked Starch Nanoparticles as a Carrier for Indomethacin and Acyclovir Drugs. *Journal of Nanomedicine & Nanotechnology*, 6(1), 1-8.
- Eloy, J., Saraiva, J., Albuquerque, S., Marchetti, J. (2012). Solid Dispersion of Ursolic acid in Gelucire®50/13 : a strategy to enhance drug release and trypanocidal Activity. *American Association of Pharmaceutical Scientists PharmSciTech*, 13(4), 1436-1445.
- Guns, S., Dereymaker, A., Kayaert, P., Mathot, V., Martens, J., Mooter, G. (2011). Comparison between hot-melt extrusion and spray-drying for manufacturing solid dispersions of the graft copolymer of ethylene glycol and vinylalcohol. *Pharmaceutical Research*, 28(3), 673-682.
- Higuchi, T. (1963) Mechanism of sustained action medication theoretical analysis of rate of release of solid drugs dispersed in solid matrices, *Journal of Pharmaceutical Sciences*, 52, 1145-1149.
- Higuchi, T., Connors, K.A. (1965). Phase solubility techniques. *Advanced Analytical Chemistry of Instrumentation*, 4, 117-212.
- Hou, D.Z., Gui, R.Y., Hu, S., Huang, Y., Feng, Z.Y., Ping, Q.N. (2015). Preparation and Characterization of Novel Drug-Inserted-Montmorillonite Chitosan Carriers for Ocular Drug Delivery. *Advances in Nanoparticles*, 4, 70- 84.
- Karavelidis, V., Karavas, E., Giliopoulos, D. (2011). Papadimitriou S, Bikiaris D. Evaluating the effect of crystallinity in new biocompatible polyester nanocarriers on drug release behavior. *International Journal of Nanomedicine*, 6, 3021-3032.
- Kaushik, A., Tiwari, A., Gaur, A. (2015). Role of excipients and polymeric advancements in preparation of floating drug delivery systems. *International Journal of Pharmaceutical Investigation*, 5(1).
- Lee, J., Lee, H., Jang, K., Lim, K.S., Shin, D., Yu, K.S. (2014). Evaluation of the pharmacokinetic and pharmacodynamic drug interactions between cilnidipine and valsartan, in healthy volunteers. *Drug, Design, Development and Therapy*, 8(8), 1781-8. doi:10.2147/DDDT.S68574.
- Lima, A.A.N., Sobrinho, J.L.S., Correa JR R.A.C., Rolim Neto, P.J. (2008). Alternative Technologies to Improve Solubility of Poorly Water Soluble Drugs. *Latin American Journal of Pharmacy*, 27(5), 789-97.
- Long, J., Etxeberria, A E., Kornelsen, C., Nand, A., Ray, S., Bunt, C., Seyfoddin, A. (2019) Development of a long-term drug delivery system with levonorgestrel loaded chitosan microspheres embedded in poly (vinyl alcohol) hydrogel. *ACS Applied Materials*, 2(7), 2766-2779, DOI: 10.1021/acsabm.9b00190 .

- Mishra, R., Mir, S.R., Amin, S. (2007). Polymeric nanoparticles for improved bioavailability of cilnidipine. *International Journal of Pharmacy and Pharmaceutical Sciences*, 9(4), 129-139.
- Mudalige, T., Qu, H., Haute, D.V., Ansar, S.M., Paredes, A., Ingle, T. (2019). Characterization of Nanomaterials: Tools and Challenges. *Nanomaterials for food applications*, chapter 11, 313-353.
- Panigrahi, K.C., Patra, N., Jena, G.K., Ghose, D., Jena, J., Panda, S.K., Sahu, M., (2017). Gelucire®50/13: A versatile polymer for modified release drug delivery system. *Future Journal of Pharmaceutical Sciences*, 1-7.
- Patel, K., Patel, M. (2014). Preparation and evaluation of chitosan microparticles containing nicorandil. *International Journal of Pharmaceutical Investigation*, 4(1), 32-37
- Peppas, N.A. (1985). Analysis of fickian and non-fickian drug release from polymers. *Pharm. Acta. Helv*, 60, 110-111.
- Pinto, I.C., Cerqueira-Coutinho, C., Freitas, Z.M.F., Santos, E.P., Carmo, F.A., Ricci Junior, E. (2017). Development and validation of an analytical method using High Performance Liquid Chromatography (HPLC) to determine ethyl butylacetylaminopropionate in topical repellent formulations. *Brazilian Journal of Pharmaceutical Sciences*, 53(2).
- Rajebahadur, M., Zia, H., Nues, A. Lee, C. (2006). Mechanistic study of solubility enhancement of nifedipine using vitamin E TPGS and Solutol HS 15. *Drug Delivery*, 13, 201-206.
- Reddy, K.V.M., Nagabhushnam, M.V. (2017). Process and parameters affecting drug release performance of prepared cross-linked alginate hydrogel beads for ezetimibe. *International Journal of Pharmacy and Pharmaceutical Sciences*, 9(2).
- Ruchatz, F., Schuch, H., (1998). Physicochemical properties of Solutol HS 15 and its solublizates, *BASF ExAct*, 6-7.
- Sareen, S., Mathew, G., Joseph, L. (2012). Improvement in solubility of poor water soluble drug by solid dispersion. *International Journal of Pharmaceutical Sciences*, 2(1), 12-17.
- Sarfraz, M.D., Hiremath, D., Choudhary, K.P.R. (2010). Formulation and characterization of rifampicin microcapsules. *International Journal of Pharmaceutical Sciences*, 72, 101-105.
- Sedyakina, N.E., Feldman, N.B., Lutsenko, S.V., Avramenko, G.V. (2018). Fabrication and drug release behavior of ionically cross-linked chitosan microspheres. *Mendeleev Communications*, 28, 598-600.
- Sharma, A., Jain, C.P. (2010). Preparation and Characterization of solid dispersions of Cavedilol with PVP K30. *Res Pharma Sci*, 5(1), 49-56.
- Siepmann, J., Elkharraz, K., Siepmann, F., Klose, D., (2005). How Autocatalysis Accelerates Drug Release from PLGA-Based microparticles: A Quantitative Treatment. *Biomacromolecules*, 6, 2312-2319.
- Solak, E.K. (2011). Preparation and characterization of interpenetrating polymeric network microspheres for controlled delivery of naproxen. *Journal of Biomaterials and Nanobiotechnology*, 2, 445-453.
- Uneyama, H., Uchida, H., Konda, T., Yoshimoto, R., Akaike, N. (1999). Selectivity of dihydropyridines for cardiac L-type and sympathetic N-type Ca²⁺ channels. *European Journal of Pharmacology*, 373(1), 93-100.
- Viveksarathi, K., Kannan, K. (2015). Effect of the moist-heat sterilization on fabricated nanoscale solid lipid particles containing rasagiline mesylate. *International Journal of Pharmaceutical Investigation*, 5(2), 87-91.